Available online at www.sciencedirect.com
ScienceDirect
Pattern Recognition Letters 28 (2007) 1209–1221
Pattern Recognition Letters
www.elsevier.com/locate/patrec

Recursive sub-image histogram equalization applied to gray scale images

K.S. Sim *, C.P. Tso, Y.Y. Tan

Faculty of Engineering and Technology, Multimedia University, Jalan Ayer Keroh Lama, Bukit Beruang, 75450 Melaka, Malaysia

Received 24 March 2006; received in revised form 5 February 2007
Available online 20 February 2007

Communicated by R. Davies

Abstract

A novel recursive sub-image histogram equalization (RSIHE) is developed to overcome the drawbacks of generic histogram equalization (HE) for gray scale images. Compared to some of the conventional HE methods, such as bi-histogram equalization and recursive mean-separate histogram equalization, the proposed RSIHE method yields better image compensation. The scanning electron microscope images are used as test images to evaluate the efficiency of the developed algorithm. The algorithm is implemented in software with a frame grabber card, forming the front-end video capture element.

Keywords: Histogram equalization; Scanning electron microscope

1. Introduction

Histogram equalization (HE) is a popular technique for enhancing image contrast (Gonzalez and Woods, 2002). The basic idea is to map the gray levels based on the probability distribution of the image input gray levels. HE flattens and stretches the dynamic range of an image histogram and gives an overall contrast improvement. In fact, HE has been applied in various areas, such as medical image processing (Du et al., 2004; John et al., 2004; Venkatachalam et al., 2004; Pizer, 2003). Furthermore, the HE method is available in most image processing packages, such as Adobe Photoshop (Weichselbaum et al., 2005), National Institutes of Health Image (Rasband and Bright, 1995), and Lispix (Bright, 1995). Anyhow, HE is not commonly used on scanning electron microscope (SEM) images because this method causes significant change on the input image brightness and introduces undesirable artifacts. Since the mean brightness of the histogram-equalized image is always the middle gray level regardless of the input image mean, this characteristic is not desirable in applications where brightness preservation is necessary (Chen and Ramli, 2003).

The mean preserving B-histogram equalization (BHE) (Kim, 1997) has been proposed to overcome the problem. First, the BHE separates the input image histogram, based on its mean value, into two parts: one ranges from the minimum gray level to the mean value, and the other, from the mean value to the maximum gray level. The generalization of BHE, namely, the recursive mean separate histogram equalization (RMSHE), has also been studied (Chen and Ramli, 2003).

During the last few decades, several approaches based on auto brightness contrast (ABC) compensation techniques have been proposed to address the undesirable artifacts. In SEM images, for example, the viewed object can become charged by the SEM electron beam when certain insulating materials are not metal coated before SEM observation (Belhaj et al., 2000; Goldstein et al., 1992). Other problems include noise, dirt, nonlinearities in the

* Corresponding author. Tel.: +606 252 3480; fax: +606 231 6552.
E-mail addresses: sksbg2003@yahoo.com, kssim@mmu.edu.my (K.S. Sim).

0167-8655/$ - see front matter © 2007 Elsevier B.V. All rights reserved.
doi:10.1016/j.patrec.2007.02.003

detector or amplifier, non-uniformity across the scene, clipping of pixels at white or black, and geometric distortion during scanning. The ABC methods have different degrees of success (Belhaj et al., 2000; Wong et al., 1995; Wong, 1997; Russ, 1999; Tolat et al., 1991; De Medeiros Martins et al., 2002); in spite of their considerable achievements, conventional ABC methods still have several constraints when the region-of-interest does not occupy a significant portion of the field-of-view. In addition, the conventional ABC techniques focused on post-processing images rather than on real-time images (Chen and Ramli, 2003).

In this paper, we propose to design a novel histogram equalization that is able to preserve the mean energy and overcome the problem facing the conventional HE methods. As test-images, we consider SEM images to evaluate the robustness of the efficiency of the developed algorithm. Several SEM test-images have been used to compare the performance of the conventional HE methods, the BHE method, the RMSHE method, and the new proposed method. The structural similarity index (SSI) (Wang et al., 2003) and the peak signal-to-noise ratio (PSNR) (Chen and Fischer, 1998; Kossentini et al., 1995) are used to analyze the image quality. To make the new technique versatile, we embed the technique onto a frame grabber card to create a real-time imaging system. A new imaging system is set up by integrating a PC with a SEM. With the new setup, we can online assess the quality of the SEM images and implement the necessary improvement.

This paper is organized as follows: Section 2 documents the histogram equalization (HE) method and analyses the HE brightness change, Section 3 presents the available HE methods and the new HE method, Sections 4 and 5 discuss the measurement tools and results, Section 6 describes the SEM hardware imaging system, and Section 7 concludes the finding.

2. Histogram equalization

Let the two-dimensional image $W(i,j)$ composed of V discrete gray levels, denoted by $\{W_0, W_1, \ldots, W_k, \ldots, W_{V-1}\}$. The probability density function (PDF) of W_k is defined as

$$PDF(W_k) = n_k/n, \tag{1}$$

where $k = 0, 1, \ldots, V-1$, $n_k =$ number of pixels that have the value of k, and n is the total number of samples.

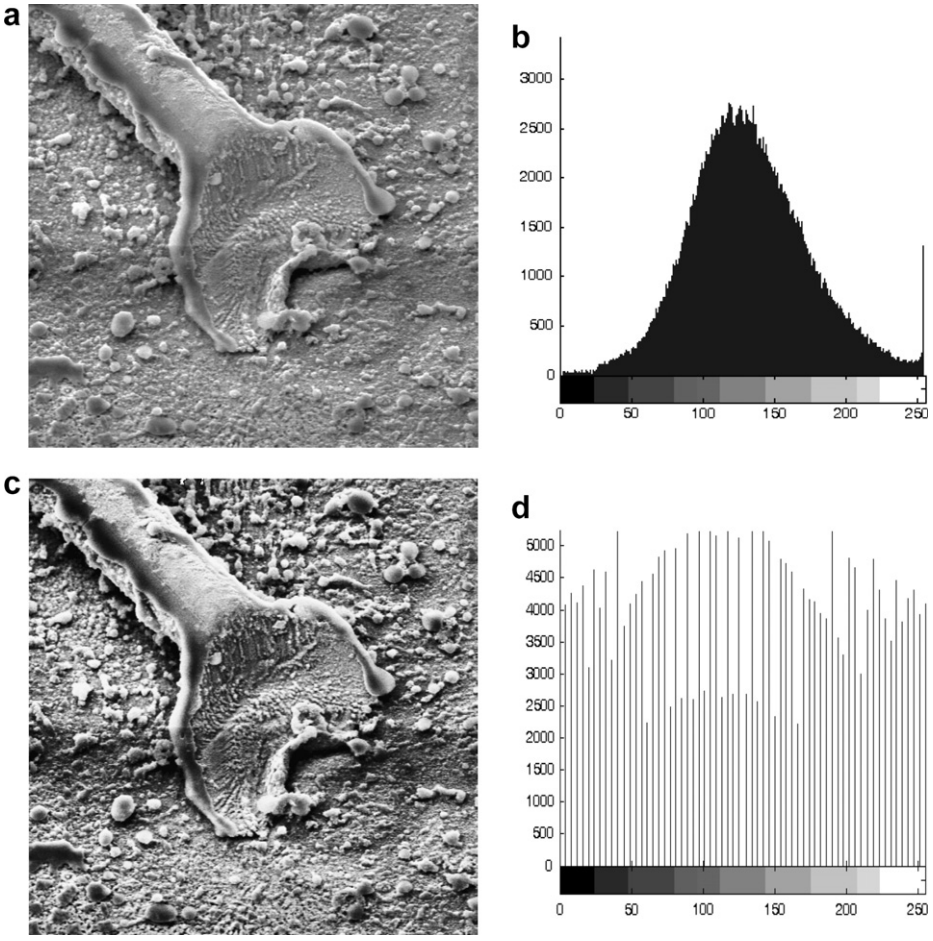

Fig. 1. A SEM sample image of a gold wire stitch bond on a lead frame and its histogram, before and after histogram equalization. Image size = 256 by 256, and the horizontal field-width = 500 μm at 20 keV.

Note that $PDF(W_k)$ is associated with the histogram of an input image that represents the number of pixels that have a specific input intensity W_k. A plot of n_k versus W_k is known as the histogram of image $W(i,j)$. Based on the PDF, the cumulative density function (CDF) is defined as

$$CDF(w) = \sum_{j=0}^{k} PDF(W_j), \tag{2}$$

where $w = W_k$, for $k = 0, 1, \ldots, V-1$. By definition, $CDF(W_{V-1}) = 1$. The histogram equalization is a design that maps the input image into the entire dynamic range (W_0, W_{V-1}).

Figs. 1a and b show a SEM image with its equivalent histogram. The output image of the gold wire stitch bond after histogram equalization is given in Figs. 1c and d. This result demonstrates the performance of the HE method in

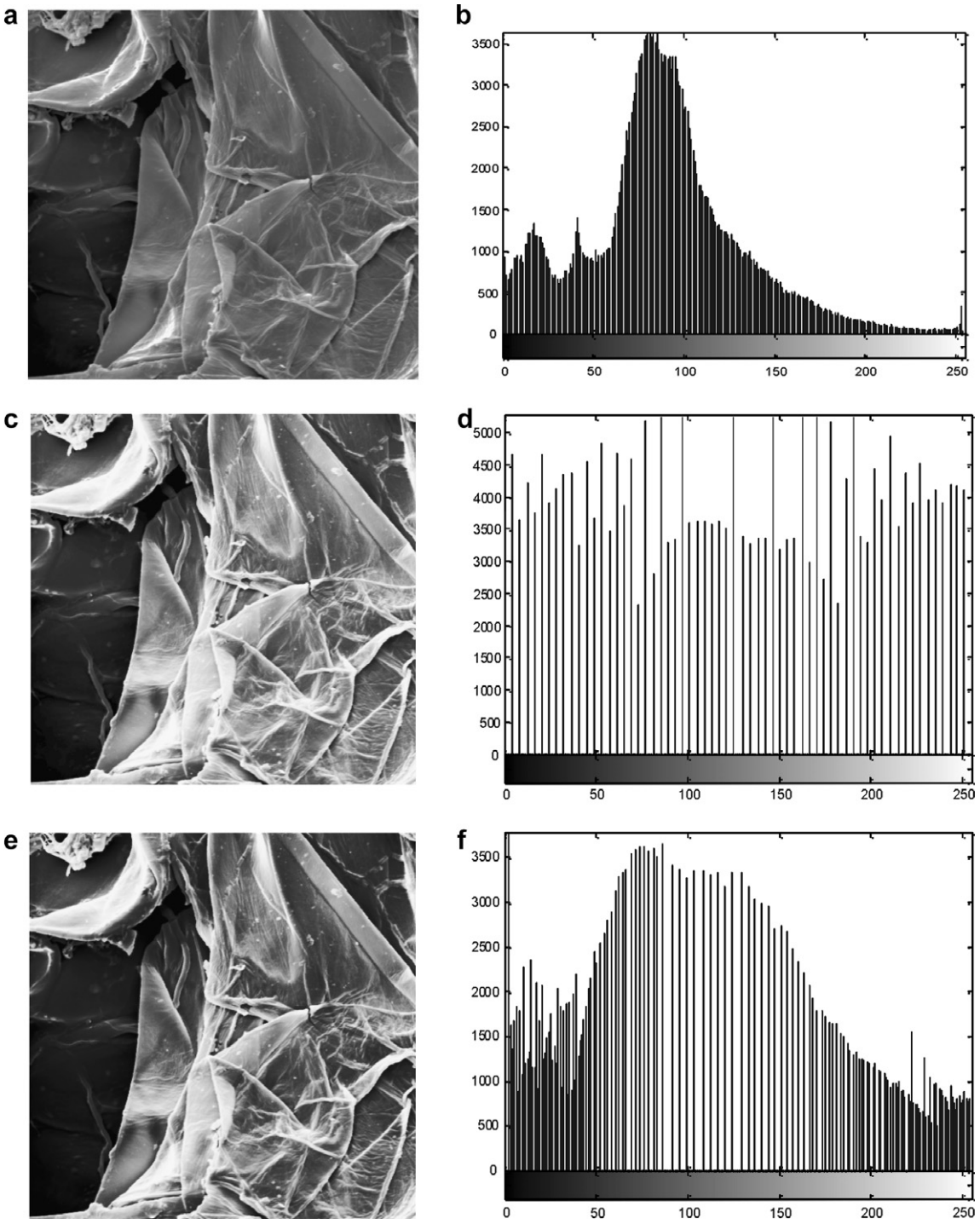

Fig. 2. The Bamboo composite sample image and its histogram with horizontal field width = 50 μm at (a), (b): original. (c), (d): after HE. (e), (f): after BHE.

enhancing the contrast of an image through dynamic range expansion.

HE can introduce a significant change in image brightness. For instance, after applying the HE method, the output image of the gold wire stitch bond on a lead-frame is much brighter than the input image. Usually, the HE maps its input to a gray level that is proportional to the cumulative density. The fundamental reason behind this limitation is that it does not take the image mean brightness into account. In the next subsection, we will show that the mean brightness of the HE method output image is the middle gray level instead of the input image mean.

2.1. Analysis on the brightness change by histogram equalization

Suppose that w is a continuous random variable; the output of the histogram equalization Z is then a random variable. It is understood that HE produces an image whose gray levels have a uniform density,

$$p(w) = 1/(W_{V-1} - W_0) \quad \text{for } W_0 \leqslant w \leqslant W_{V-1}. \tag{3}$$

Thus, the mean brightness of the output image after HE is

$$E(Z) = \int_{W_0}^{W_{V-1}} wp(w)\,\mathrm{d}w = \frac{(W_{V-1} + W_0)}{2}, \tag{4}$$

where $E(\cdot)$ denotes a statistical expectation. It shows that the mean brightness of the HE output image the middle gray level and has no relationship with the input image mean. Obviously, this property is undesirable in many image-processing applications; this property, indeed, expresses the limitation of HE images, whether the images are captured under dark or bright environment. More examples will be discussed in the following sections.

3. Available HE methods

Besides the conventional HE methods, there are two other types of methods: the BHE and the RMSHE methods. In this section, we would discuss the two methods.

3.1. Bi-histogram equalization

The BHE is used to lessen the drawback of the conventional HE method, which is unable to preserve the original image brightness; the brightness is important because it helps to minimize any visual deterioration due to histogram modification, and reduce the occurrence of artifacts.

First, BHE divides an input image into two sub-images based on the mean of the input image. Equalizations are later performed independently for the two sub-images.

Fig. 2 shows output images of a Bamboo composite sample image before applying the BHE method (in Fig. 2a) onto it, after applying the HE method (in Fig. 2c), and after the BHE method (in Fig. 2e).

The BHE can achieve brightness preservation because it performs mean-separation before any histogram equalization. Mean-separation refers to the separation of an input image into sub-images. In the conventional HE method, there is no mean-separation; thus, there is no brightness preservation. HE transforms a darker image into a brighter image; this result is portrayed in Fig. 2.

We would also like to preserve the image contrast. That is, if there is a difference in brightness, we want to preserve it so that we can see it. Microscopes provide a waveform view so that we can see the range of brightness in an image. Nevertheless, a signal outside that range will be clipped and only registered as fully white or black, thereby losing details in those regions (Goldstein et al., 1992).

3.2. Recursive mean-separate histogram equalization

The performance of RMSHE is claimed to be better in some cases where HE and BHE fail in their applications.

In BHE, mean-separation is done once; therefore, there is brightness preservation in certain situations. Chen and Ramli (2003) explain that if more mean-separations are done recursively, more brightness preservation can be achieved. Fig. 3 exhibits the image of the IC compound filler sample image captured from SEM with horizontal field-width 50 μm at 10 keV.

In Fig. 4, r, the recursive level for RMSHE, is equal to 0 because in typical HE, there is no mean-separation. Equalization is performed over the entire dynamic range ($W_0 = 0$ to $W_{V-1} = 255$).

In Fig. 5a, r is equal to 1 because the mean-separation is performed once in BHE, and equalizations are executed on its sub-images. Fig. 5a displays two regions with two bounding boxes, with intensity level = 119 as its mean, denoted by W_m. The first region (W_0, W_m) is the sub-image W_L, and the second region (W_{m+1}, W_{V-1}) is the sub-image W_U.

For RMSHE with $r = 2$, the input image $W(i,j)$ is separated into four sub-images by mean-separation, as shown in Fig. 6a. It is divided based on W_m and then further divided into two respective sub-images: W_L and W_U. $W_{lm} = 91$ and $W_{um} = 155$ are the means of W_L and W_U,

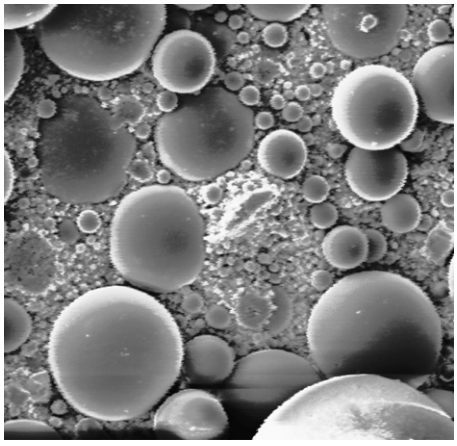

Fig. 3. The IC compound filler sample image captured from SEM with horizontal field-width = 50 μm.

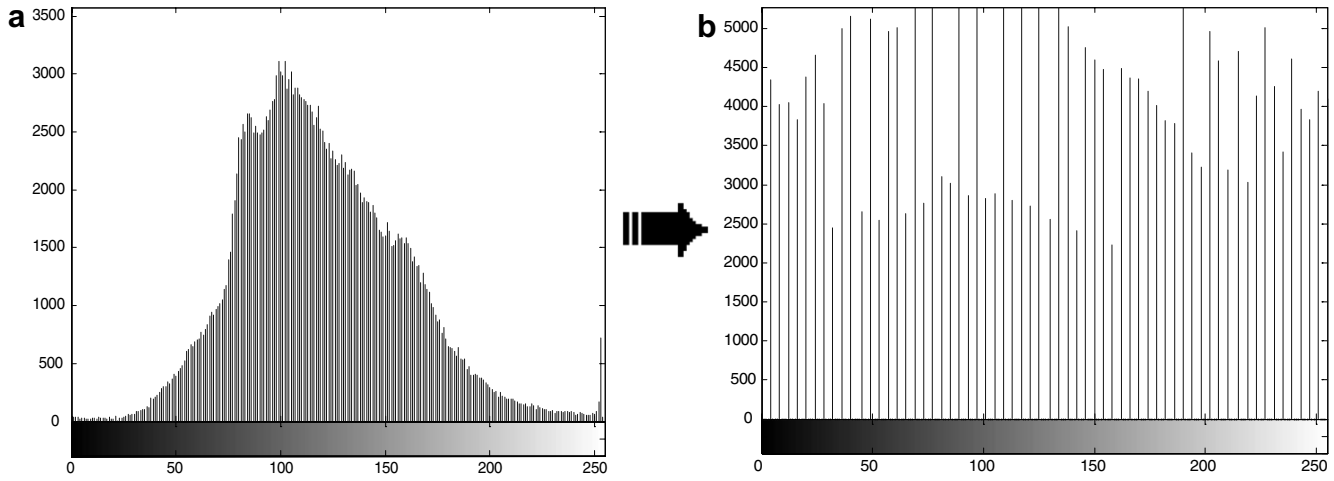

Fig. 4. Histogram of original image at (a) and histogram of IC compound filler sample image after applied HE (RMSHE, $r = 0$) at (b).

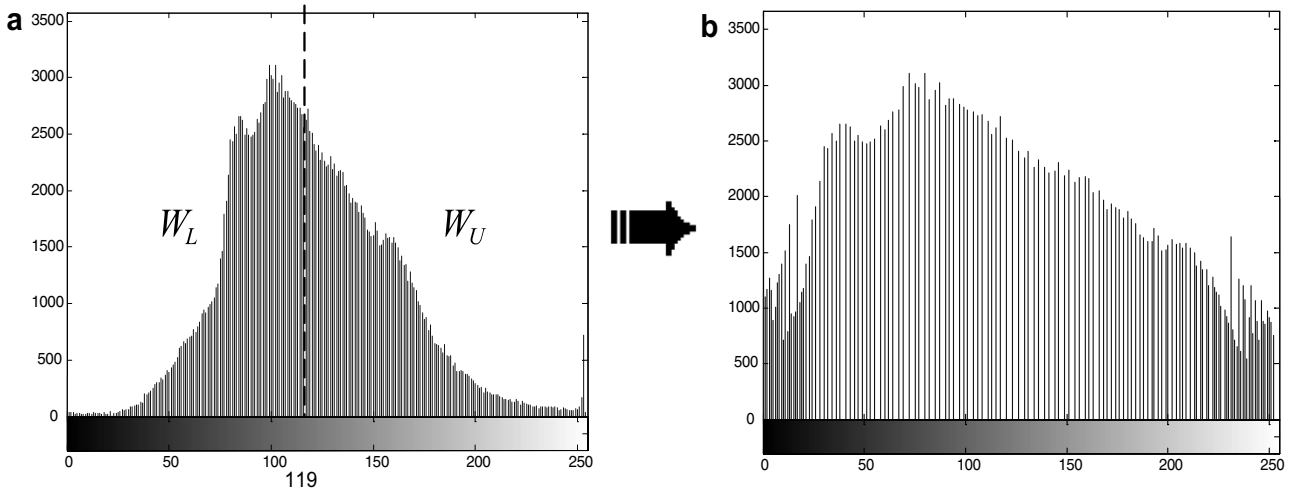

Fig. 5. Histogram representation of the BHE. (a) Original histogram of IC compound filler sample image. (b) Histogram of (a) after BHE (RMSHE, $r = 1$).

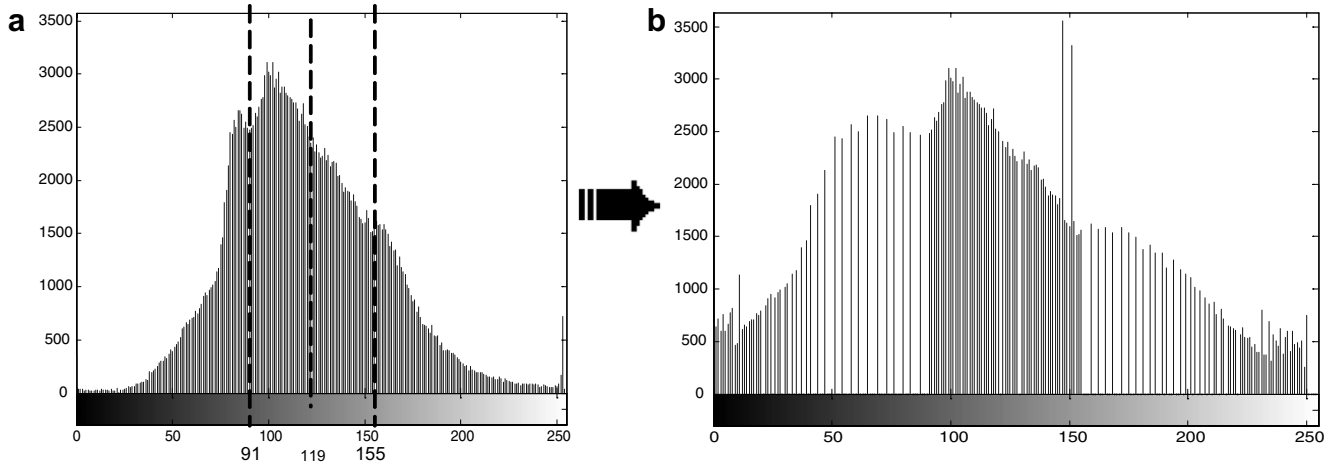

Fig. 6. Histogram representation of RMSHE. (a) Original histogram of IC compound filler sample image. (b) Histogram of (a) after RMSHE, $r = 2$.

respectively. $W(i,j)$ is expressed as the combination of the four sub-images.

3.3. Novel recursive sub-image histogram equalization

We now propose an equalization method called recursive sub-image histogram equalization (RSIHE). RSIHE and RMSHE share the same characteristics in equalizing an input image sub-images, except that RSIHE chooses to separate the histogram based on gray level with cumulative probability density equal to 0.5, but RMSHE uses mean-separation approach discussed in Section 3.2. When cumulative probability density is equal to 0.5, the total pixels in a sub-image, say W_U, and the total pixels in the other sub-image, say W_L, are the same.

The intermediate value, W_m, can be determined using the cumulative probability density function for the gray level W_k equals to 0.5. An image $W(i,j)$ can then be separated into its corresponding sub-images based on the calculated W_m.

The input image W can be decomposed into the two sub-images, namely, W_L and W_U, where W_L consists of $\{W_0, W_1, \ldots, W_m\}$ and W_U consists of $\{W_{m+1}, W_{m+2}, \ldots, W_{V-1}\}$. Next, the PDFs of the sub-images W_L and W_U are defined as

$$PDF_L(W_k) = \frac{n_{Lk}}{n_L}, \tag{5}$$

where n_L is the total numbers of pixels in W_L, n_{Lk} is the total numbers of pixels with gray-level in W_k, and $k = 0, 1, \ldots, m$.

$$PDF_U(W_k) = \frac{n_{Uk}}{n_U}, \tag{6}$$

where n_U is the total numbers of pixels in W_U, n_{Uk} is the total numbers of pixels with gray-level in W_k, and $k = m+1, m+2, \ldots, V-1$.

In the next step, the CDF is defined for both sub-images:

$$CDF_L(W_k) = \sum_{i=0}^{k} PDF_L(W_i), \tag{7}$$

where, $k = 0, 1, \ldots, m$ and

$$CDF_U(W_k) = \sum_{i=m+1}^{k} PDF_U(W), \tag{8}$$

where, $k = m+1, m+2, \ldots, V-1$.

The transformed functions $f_L(w)$, using the CDF derived from Eqs. (7) and (8), are defined as below:

$$f_L(w) = W_0 + (W_m - W_0) CDF_L(w), \tag{9}$$

and

$$f_U(w) = W_{m+1} + (W_{L-1} - W_{m+1}) CDF_U(w). \tag{10}$$

Finally, the output image of the RSIHE, Z, is expressed as $f_L(W_L)$ and $f_U(W_U)$.

From Eqs. (9) and (10), the histogram is divided into two equalized sub-images. In order to have more sub images, we make use of Eq. (11):

$$S = 2^r, \tag{11}$$

where S is the number of sub-images to be equalized, r is the recursive level for the RSIHE.

Again the histogram of IC compound filler sample image is used in Fig. 7. From Fig. 7a, we observe that the number of pixels in sub-image W_L approximate the number of pixels in sub-image W_U. Equalization is performed on both sub-images, W_L and W_U, respectively.

When $r = 2$, the RSIHE separates image $W(i,j)$ into four sub-images, namely $W_{\text{sub1}}, W_{\text{sub2}}, W_{\text{sub3}}$, and W_{sub4}.

Let N_W be the total number of pixels in image W; then, $N_{W_{\text{1sub}}}, N_{W_{\text{sub2}}}, N_{W_{\text{3sub3}}}$, and $N_{W_{\text{4sub}}}$ are the total number of pixels correspond to sub-images $W_{\text{sub1}}, W_{\text{sub2}}, W_{\text{sub3}}$, and W_{sub4}, respectively.

From Fig. 8a, the histogram is divided into four equal-area sub-images. The histogram equalization is then

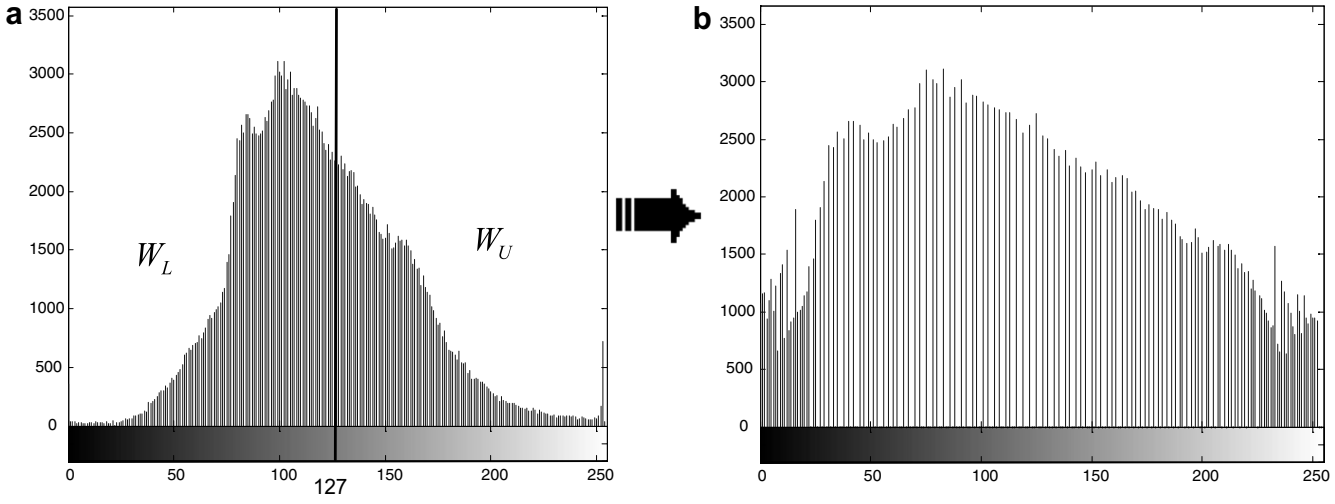

Fig. 7. Histogram representation of the RSIHE. (a) Original histogram of IC compound filler sample image. (b) Histogram of (a) after the RSIHE, $r = 1$.

applied to the four sub-images. The key factor for the RSIHE is to determine the intermediate values of its sub-images. From Eq. (2), we have

$$CDF(I_K) \cong 0.25, \text{ then } I_K = I_1,$$

$$CDF(I_K) \cong 0.50, \text{ then } I_K = I_2,$$

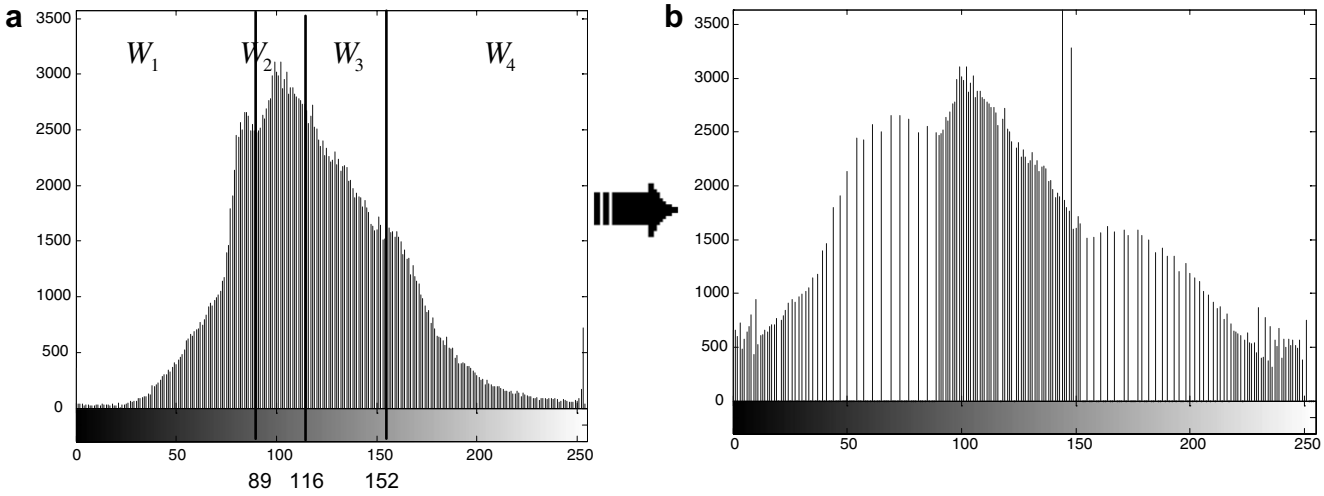

Fig. 8. Histogram representation of the RSIHE. (a) Original histogram of IC compound filler sample image. (b) Histogram of (a) after RSIHE, $r = 2$.

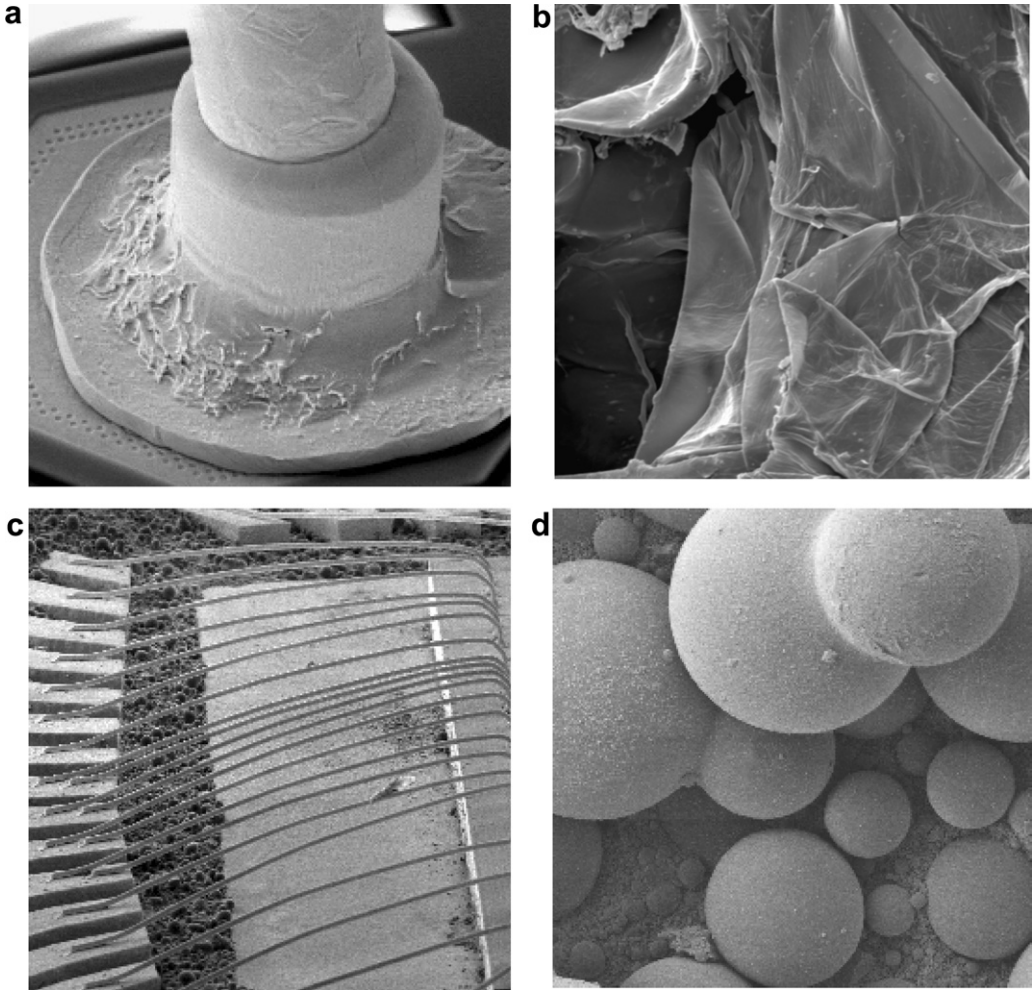

Fig. 9. SEM images taken at slow scan rate: (a) Wire bonding IC sample with horizontal field width = 20 μm, (b) bamboo composite sample with horizontal field width = 50 μm, (c) Logic IC sample with horizontal field width = 3 mm, and (d) IC compound filler sample with horizontal field width = 100 μm.

and

$$CDF(I_K) \cong 0.75, \text{ then } I_K = I_3,$$

where I_1, I_2, I_3 are the intermediate values for splitting image W into its sub-images.

In addition, the RSIHE could be further enhanced by splitting any image into n equal-area sub-images, where n ranges from 2 to 8. This ability gives the RSIHE method an advantage of scalable brightness preservation. The value of n is proposed to be less than or equal to 8, because having too many sub-images can result in ineffective image enhancement. Moreover, more sub-images consumes more computation time.

3.4. Analysis for the brightness change by RSIHE

Suppose that the gray level distribution probability of the output image using RSIHE with $r = 2$ is

$$\begin{aligned}&\{p_i | i = 0, 1, \ldots, ml - 1\} \cup \{p_j | j = ml, ml + 1, \ldots, m - 1\}\\ &\quad \cup \{p_k | k = m, m + 1, \ldots, mu - 1\}\\ &\quad \cup \{p_n | n = mu, mu + 1, \ldots, v - 1\},\end{aligned}$$

and

$$p_i = 1/2(W_{ml-1} - W_0), \quad p_j = 1/2(W_{m-1} - W_{ml}),$$
$$p_k = 1/2(W_{mu-1} - W_m) \quad \text{and} \quad p_n = 1/2(W_{v-1} - W_{mu}).$$

The average brightness of the output image is

$$\begin{aligned}E(Z) &= E(Z|W < W_{ml}) + E(Z|W_{ml} \leqslant W < W_m)\\ &\quad + E(Z|W_m \leqslant W < W_{mu}) + E(Z|W_{mu} \leqslant W < W_{v-1})\\ &= (W_0 + W_{ml})/8 + (W_{ml} + W_m)/8\\ &\quad + (W_m + W_{mu})/8 + (W_{mu} + W_{v-1})/8\\ &= (W_{ml} + W_m + W_{mu} + (W_{v-1} + W_0)/2)/4 \qquad (12)\end{aligned}$$

We see that the average brightness of the output image using RSIHE is the average of the segmentation gray level and the middle gray level of the image gray scale. Thus, the average brightness of the original image can be maintained such that the mean of the image energy is preserved. The RSIHE implementation pseudocode is given in Appendix A.

Similarly, for the n equal sub-images, the average brightness of the output image using RSIHE is the average of the

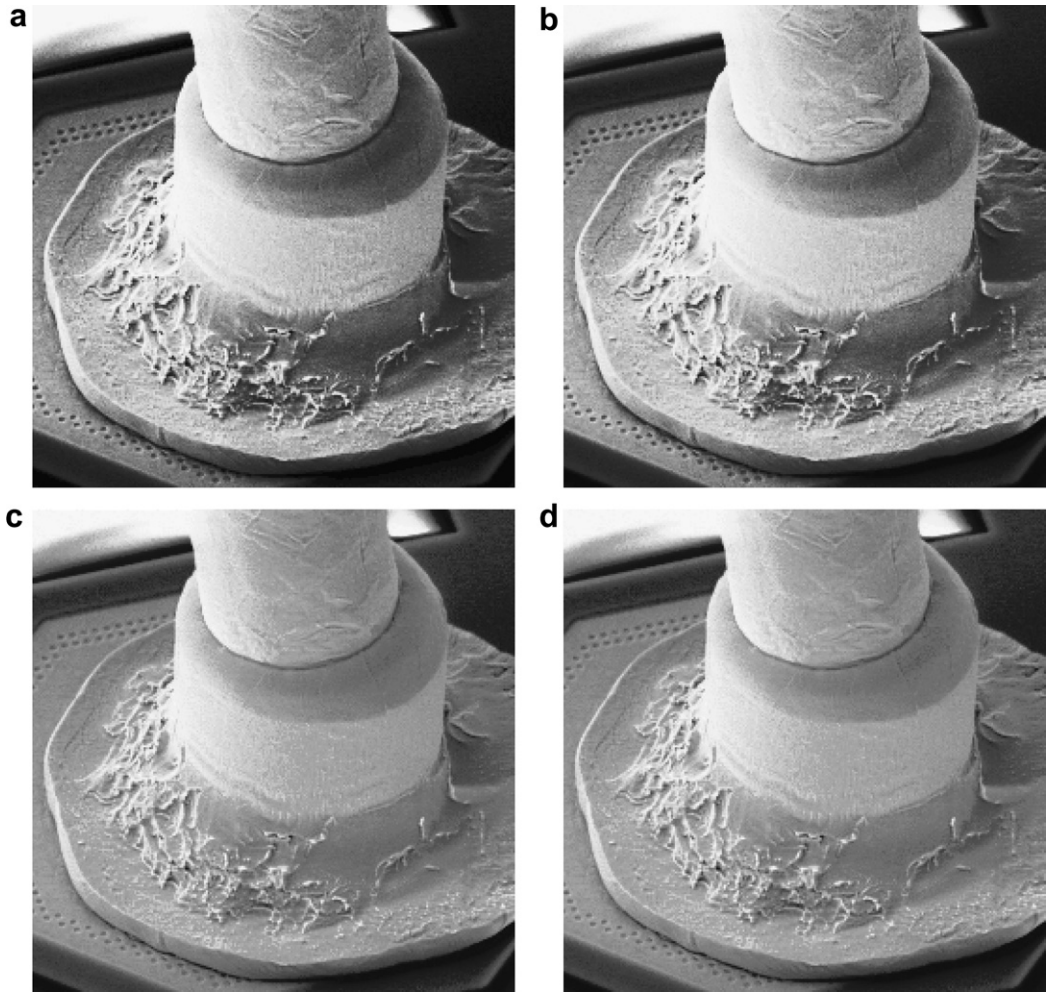

Fig. 10. Wire bonding IC sample images with horizontal field width = 20 μm at (a) after applying HE technique, at (b) after applying BSE technique, at (c) after applying RMSHE technique, and finally (d) after applying RSIHE with $n = 2$.

segmentation gray level and the middle gray level of the image gray scale.

For our application, we choose $n = 2$, without losing any generality, as it is then simple and easy to implement the recursive sub-image histogram equalization.

4. Measurement tools to assess image quality

In this section, we apply statistical parameters to assess the after-enhancement image quality.

4.1. Mean structural similarity index

We first introduce the structural similarity index (SSI) to assess the image quality:

$$SSI(x,y) = \frac{(2\mu_x\mu_y + C_1)(2\sigma_{xy} + C_2)}{(\mu_x^2 + \mu_y^2 + C_1)(\sigma_x^2 + \sigma_y^2 + C_2)}, \tag{13}$$

where μ_x is the mean of image x, μ_y is the mean of image y, σ_x is the standard deviation of image x, σ_y is the standard deviation of image y, σ_{xy} is the square root of covariance of images x and y, and C_1 and C_2 are constants. The mean SSI is

$$MSSI(X,Y) = \frac{1}{M}\sum_{i=1}^{M} SSI(x_i, y_i) \tag{14}$$

where X and Y are the reference and the reconstructed images, respectively; x_i and y_i are the image contents at the ith local window; and M is the number of local windows of the image.

4.2. Peak signal-to-noise ratio

For the peak signal-to-noise ratio (PSNR), we assume a source image $X(i,j)$ that contains M by N pixels and a reconstructed image $Y(i,j)$, where Y is reconstructed by decoding the encoded version of X (i,j). Errors are computed only on the luminance signal; so, the pixel values $X(i,j)$ range between black (0) and white (255).

First we compute the mean squared error (MSE) of the reconstructed image as follows:

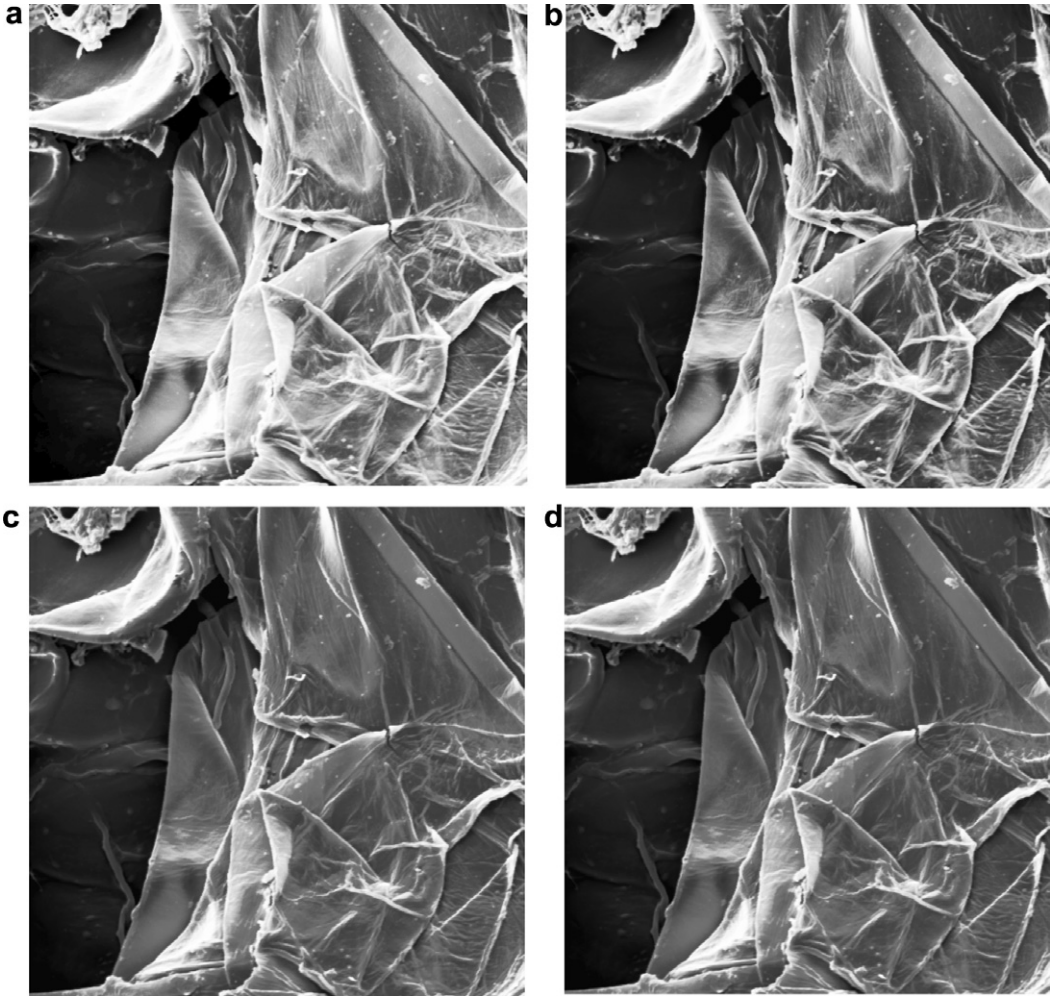

Fig. 11. Bamboo composite sample images with horizontal field width = 50 μm at (a) after applying HE technique, at (b) after applying BSE technique, at (c) after applying RMSHE technique, and finally (d) after applying RSIHE with $n = 2$.

$$MSE = \frac{\sum_{i=1}^{M}\sum_{j=1}^{N}[X(i,j) - Y(i,j)]^2}{M \times N} \quad (15)$$

The summation is over all pixels. The root mean squared error (RMSE) is the square root of MSE. Then the PSNR in decibels (dB) is computed as

$$PSNR = 20\log_{10}\left(\frac{\max(Y(i,j))}{RMSE}\right) \quad (16)$$

5. Results

To demonstrate the performance of the proposed RSIHE method in preserving and improving the quality of SEM images, we show four different SEM images, as presented in Fig. 9. We apply the RSIHE method and compare its performance with the conventional HE, BHE, and RMSHE methods; the results are produced in Figs. 10–13, respectively. To assess the quality of the processed images, we use criteria based on MSSI and PSNR. Furthermore, the improvements are deducible only from measures such as those given in Tables 1 and 2.

In the first experiment, the wire bonding IC sample image with horizontal field width equal to 20 μm is applied with the various methods. The results are shown in Fig. 10. From Table 1, we see that after the application of RSIHE, the image has the highest MSSI, showing that the RSIHE method provides not only better brightness preservation, but also highest structure similarity. The features that lead to the success of RSIHE are energy preservation, better contrast, and high PSNR and MSSI images. For this example, the SEM captured images are seen to be highly structured. Their pixels exhibit strong dependencies, especially when they are spatially proximate; these dependencies carry important information about the structure of the objects in the visual scene. Furthermore, the MSSI is a measure of the structural information change that can furnish one with a good approximation to perceived image formation. Sometimes it is difficult to visualize through the naked eyes the difference between images. However, in the later part of this section, with the criteria based on the MSSI and PSNR, we are able to point out that the RSIHE method is better than the other methods.

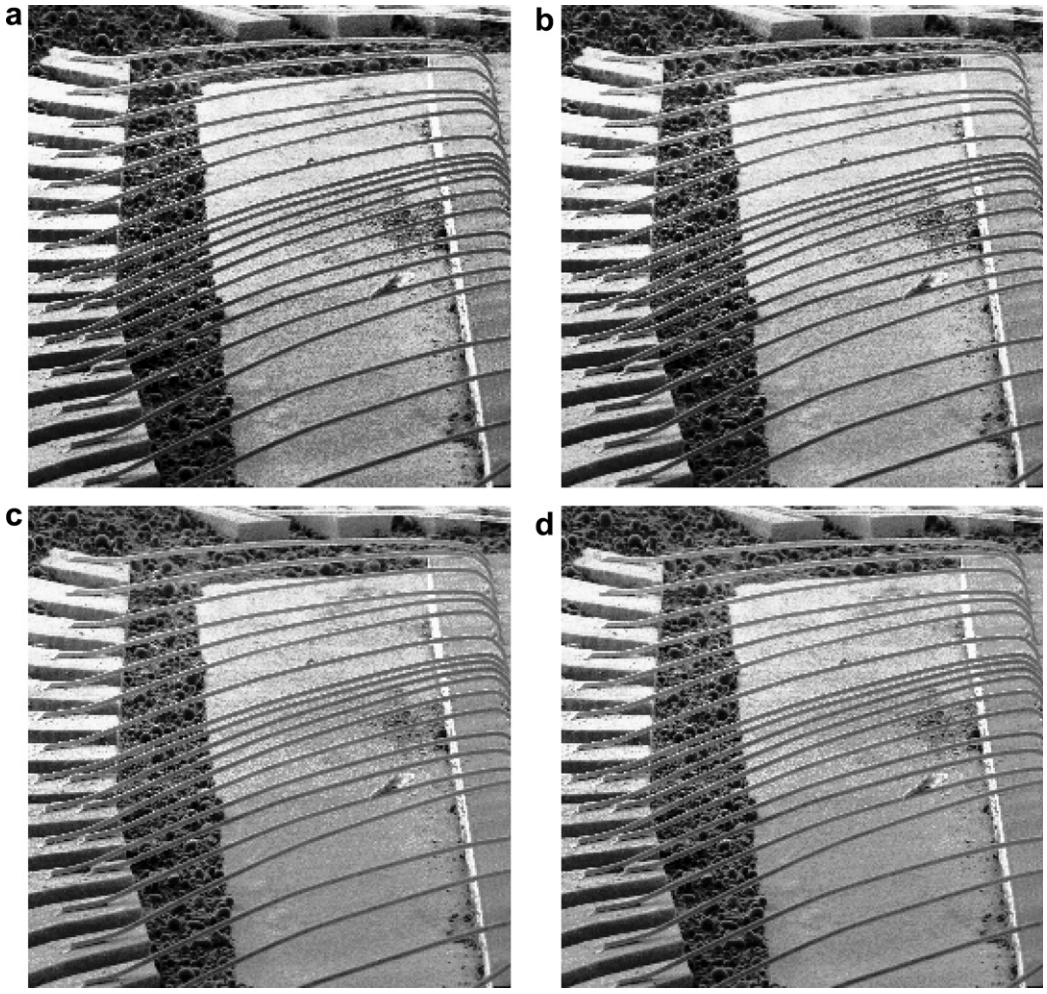

Fig. 12. Logic IC sample images with horizontal field width = 3 mm at (a) after applying HE technique, at (b) after applying BSE technique, at (c) after applying RMSHE technique, and finally (d) after applying RSIHE with $n = 2$.

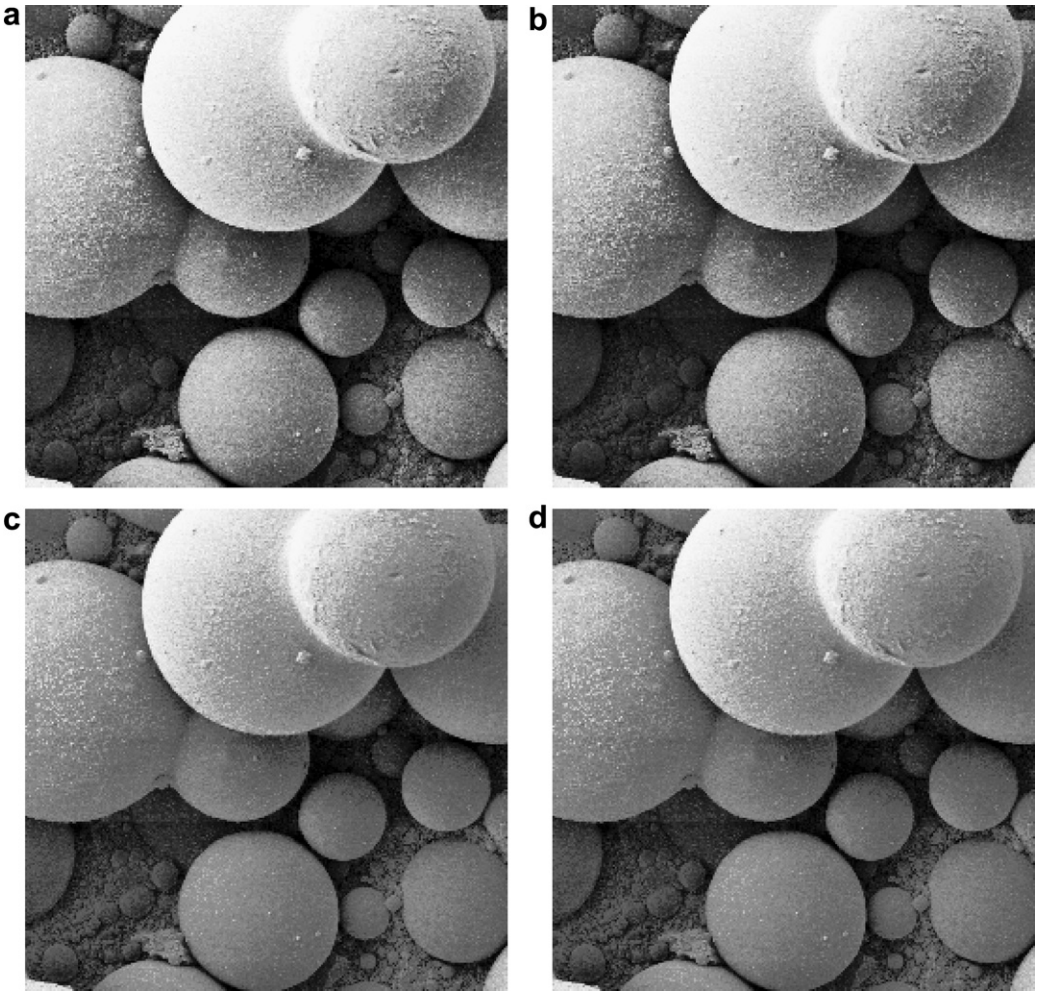

Fig. 13. IC compound filler sample images with horizontal field width = 100 μm at (a) after applying HE technique, at (b) after applying BSE technique, at (c) after applying RMSHE technique, and finally (d) after applying RSIHE with $n = 2$.

Table 1
MSSI obtained by applying Eq. (14)

Image	MSSI			
	HE	BHE	RMSHE	RSIHE
Wire bonding IC sample image	0.7768	0.8148	0.9618	0.9682
Bamboo composite material sample image	0.7625	0.7640	0.9339	0.9332
Logic IC sample image	0.8586	0.8895	0.9702	0.9735
IC compound filler sample image	0.7374	0.7409	0.8803	0.8806

Table 2
Peak signal-to-noise ratio obtained by applying Eq. (16)

Image	Peak signal-to-noise ratio (dB)			
	HE	BHE	RMSHE	RSIHE
Wire bonding IC sample image	18.20	19.06	29.06	30.34
Bamboo composite material sample image	13.51	15.68	13.15	19.60
Logic IC sample image	19.69	20.05	26.16	26.81
IC compound filler sample image	16.62	17.22	22.70	22.80

In the second experiment we use the bamboo composite sample image with horizontal field width equal to 50 μm for the comparison. The image contains structured clear signal to show the layout of bamboo material. Fig. 11 clearly shows the improvement in image quality obtained by RSIHE. The RSIHE image is more natural compared to those from other methods (shown in Fig. 11).

In the third experiment with the logic IC sample image, we see the layout of different materials. The image is applied with the various methods. The performance of the four techniques is shown in Fig. 12, and Figs. 12a and b contain obvious image fluctuation. Also, the structural layout of the pins is clearly shown in Figs. 12c and d.

In the fourth experiment, the IC compound filler sample image with horizontal field width equal to 100 μm is used as an example. Fig. 13d shows that the RSIHE image gives a clear difference between the filler to filler; also, it looks more natural compared with the rest of the images in Fig. 13.

To further show the better performance of the proposed RSIHE, we use the developed criteria in both Eqs. (14) and (16) to assess the quality of the processed images. The results are given in Tables 1 and 2.

The wire bonding results, shown in Fig. 10 and Table 1, shows that the MSSI values of RSIHE and RMSHE are close to 1 and marginally close to each other. Unlike other methods, RSIHE and RMSHE give lower than 0.8 MSSI values. The reason for this difference is that their image structures after applying HE and BHE are different from those in the original image. This result shows that both images after RSIHE and RMSHE preserve the quality of images. The same argument applies to the PSNR, as shown in Table 2. Compared to the other methods, RSIHE has higher PSNR; this result shows quantitative and qualitative improvements.

For Figs. 11c and d, the MSSI value is close to 1, as shown in Table 1. However, after RSHIE, the image quality is still better in terms of signal-to-noise ratio.

Fig. 12 and Table 1 show that comparing to other methods, RSIHE has MSSI value that is among the highest. This result again shows that both images after RSIHE, preserve and maintain the image quality. The same argument applies to the PSNR values, as shown in Table 2. The RSIHE has the highest PSNR.

For the silver paint sample image in Fig. 13, Table 1 shows that the MSSI values of RSIHE and RMSHE are higher. Besides, as shown in Table 2, RSIHE has the highest PSNR value.

6. Hardware implementation

The SEM is interfaced with a PC through a high performance 16-bit variable scan frame grabber card DT3152. A PC system using Pentium 4/3.2 GHz microprocessor and RAM of 1 GByte is used with SEM JEOL 840A.

MATLAB 7.0 is used as the computational platform, whereas the Microsoft C++ dynamic link library (DLL) is used for the necessary interfacing work between the PC programming interface and the frame grabber card. The developed Graphic User Interface performs the required interfacing between the frame grabber card DT3152 and MATLAB RSIHE algorithm.

7. Conclusions

Histogram equalization is a simple and effective image enhancing technique. However, in some cases, it tends to change significantly the brightness of an image. In this paper, we have looked into different improved contrast enhancement techniques, based on histogram equalization, to overcome the problem. Among all the techniques discussed, the RSIHE is the most robust, due to its recursive nature and scalable brightness preservation. The crucial features that led to the success of RSIHE are energy preservation, better contrast, and better images with high PSNR and MSSI. Their pixels exhibit strong dependencies, especially when they are spatially proximate; these dependencies carry important information about the structure of the objects in the visual scene. Furthermore, the MSSI is a measure of structural information change that can provide a good approximation to perceived image formation. Since the variety of images involved in real applications is often too broad to be covered with only a specific level of brightness preservation, the scalability in this algorithm is welcome. This property allows scaling in the brightness preservation degree to depend on the images themselves. Future work includes the testing the BHE, RSMSE, and RSIHE techniques on colored and real-time images, and determining the optimum-output technique.

Appendix A. The pseudo-code of recursive sub-image histogram equalization to gray scale image

(1) SET [A B] to the number of rows and columns (M-by-N) in image I.
(2) SET H as the histogram for the intensity image I.
(3) DISPLAY the histogram H.
(4) SET norm_H as the probability distribution function of histogram H.
(5) CALCULATE bin size of histogram H and SET it as bin size.
(6) SET low to 0;
(7) SET high to 0;
(8) SET C to cumulative sum of norm_H.
(9) SET diff to absolute difference of C and 0.5.
(10) CALCULATE the middle value of histogram image I and SET as mid.
(11) FOR all the pixel at the lower half of the histogram
    SET prob_low as the product of norm_H(i)* (i−1)
    ADD prob_low with prob_low from i−1 and SET as low
    END
(12) SET mid_lower as lower bound of middle value of histogram image I.
(13) FOR all the pixel at the upper half of the histogram
    SET prob_up as the product of norm_H(i)* (i−1)
    ADD prob_up with prob_up from i−1 and SET as up
    END
(14) SET cum_lower as the lower bound of cumulative distribution function by using cumulative sum function.
(15) SET cum_upper as the upper bound of cumulative distribution function by using cumulative sum function.
(16) SET cum_quarter1 as cumulative distribution function for X(0) to X(l) by using cumulative sum function.
(17) SET cum_quarter2 as cumulative distribution function for X(l+1) to X(m) by using cumulative sum function.
(18) SET cum_quarter3 as cumulative distribution function for X(m+1) to X(U) by using cumulative sum function.

(19) SET cum_quarter4 cumulative distribution function for X(U+1) to X(L−1) by using cumulative sum function.
(20) FOR all the pixel from pixel no.1 to mid_lower of the histogram
SET newgray(i) as unsigned 8-bit integers converted from the elements of the product of lower bound of middle value and cum_quarter1.
END
(21) SET s as the lower bound of middle value.
(22) FOR all the pixel from mid_lower to mid of the histogram
SET newgray(i) as unsigned 8-bit integers converted from the elements of the addition of s with product of (mid –s) and cum_quarter2.
END
(23) SET t as the middle value of histogram.
(24) FOR all the pixel from mid to mid_upper of the histogram
SET newgray(i) as unsigned 8-bit intergers converted from the elements of the addition of t with product of middle_upper-t and cum_quarter3.
END
(25) SET u as the upper bound of middle value.
(26) FOR all the pixel from mid_upper to the end
SET newgray(i) as unsigned 8-bit intergers converted from the elements of the addition of u with product of binsize-1-u and cum_quarter4.
END
(27) FOR each row of element image I
FOR each column of element image I
ADD one to each pixel and SET it as temp(i,j)
APPLY cdf to the image data and SET it as aa(I,j)
END
END

References

Belhaj, M., Jbara, O., Odof, S., Msellak, Rau E.L., Andrianov, M.V., 2000. An anomalous contrast in scanning electron microscopy of insulators: the Pseudo-Mirror Effect. Scanning 22, 352–356.

Bright, D.S., 1995. MacLispix: a special purpose public domain image analysis program for the Macintosh. Microbeam Analysis 4, 151–163.

Chen, Q., Fischer, T.R., 1998. Image coding using robust quantization for noisy digital transmission. IEEE Transaction on Image Processing 7 (4), 496–505.

Chen, S.D., Ramli, A.R., 2003. Contrast enhancement using recursive mean-separate histogram equalization for scalable brightness preservation. IEEE Transactions on Consumer Electronics 49 (4), 1301–1309.

De Medeiros Martins, A., Torres de Almeida Filho, W., Medeiros Brito Jr. A., Duarte Doria Neto, A., 2002. A new method for multi-texture segmentation using neural networks, Neural Networks, 2002. In: IJCNN'02. Proceedings of the 2002 International Joint Conference on, vol. 3, pp. 2064–2069.

Du, J., Fain, S.B., Gu, T.L., Grist, T.M., Mistretta, C.A., 2004. Noise reduction in MR angiography with nonlinear anisotropic filtering. Journal of Magnetic Resonance Imaging 19 (5), 632–639.

Goldstein, J.L., Newburry, D.E., Echlin, P., Joy, D.C., Romig, J.R., Lyman, A.D., Fiori, C.E., Lifshin, E., 1992. Scanning Electron Microscopy and X-Ray Microanalysis: A Text for Biologist Material Scientist and Geologist, second ed. Plenum Press, New York.

Gonzalez, R.C., Woods, R.E., 2002. Digital Image Processing. Prentice-Hall, New Jersey.

John, A., Huda, W., Scalzetti, E.M., Ogden, K.M., Roskopf, M.L., 2004. Performance of a single lookup table (LUT) for displaying chest CT images. Academic Radiology 11 (6), 609–616.

Kim, Y.T., 1997. Contrast enhancement using brightness preserving bi-histogram equalization. IEEE Transactions on Consumer Electronics 43 (1), 1–8.

Kossentini, F., Smith, M.J.T., Barnes, C.F., 1995. Image coding using entropy-constrained residual vector quantization. IEEE Transactions on Image Processing 4 (10), 1349–1357.

Pizer, S.M., 2003. The medical image display and analysis group at the University of North Carolina: Reminiscences and philosophy. IEEE Transactions on Medical Imaging 22 (1), 2–10.

Rasband, W.S., Bright, D.S., 1995. NIH Image: a public domain image processing program for the Macintosh. Microbeam Analysis Society Journal 4, 137–149.

Russ, J.C., 1999. The Image Processing Handbook. CRC Press, Florida.

Tolat A.R., McNeill S.R., Sutton M.A., 1991. Effects of contrast and brightness on subpixel image correlation. In: System Theory Proceedings, Twenty-Third Southeastern Symposium on 10–12 March, pp. 604–608.

Venkatachalam, P.A., Mohd Hani, A.F., Ngah, U.K., Lim, E.E., 2004. Processing of abdominal ultrasound images using seed based region growing method. Proceedings of International Conference on Intelligent Sensing and Information Processing, 57–62.

Wang, Y., Li, J., Lu, Y., Fu, Y., Jiang, Q., 2003. Image quality evaluation based on image weighted separating block peak signal to noise ratio. In: Neural Networks and Signal Processing, 2003. Proceedings of the 2003 International Conference on, Volume 2, pp. 994–997.

Weichselbaum, M., Sparrow, M.P., Hamilton, E.J., Thompson, P.J., Knight, D.A., 2005. A confocal microscopic study of solitary pulmonary neuroendocrine cells in human airway epithelium. Respiratory Research 6 (115), 1–11.

Wong, W.K., 1997. Control of specimen charging in scanning electron microscopy. Ph.D. Thesis, National University of Singapore, Singapore.

Wong, W.K., Phang, J.C.H., Thong, J.T.L., 1995. Charging control using pulsed electron microscopy. Scanning 17 (5), 312–315.